Hindawi Publishing Corporation
Science and Technology of Nuclear Installations
Volume 2013, Article ID 763175, 9 pages
http://dx.doi.org/10.1155/2013/763175

Research Article

Online Fatigue-Monitoring Models with Consideration of Temperature Dependent Properties and Varying Heat Transfer Coefficients

HengLiang Zhang,[1] Shi Liu,[2] Danmei Xie,[1] Yangheng Xiong,[1] Yanzhi Yu,[1] Yan Zhou,[1] and Rui Guo[1]

[1] *Wuhan University, Wuhan 430072, China*
[2] *GPGC Electric Power Research Institute, Guangzhou 510080, China*

Correspondence should be addressed to HengLiang Zhang; zhl8111@sina.com

Received 27 August 2013; Accepted 11 November 2013

Academic Editor: Bing Li

Thermal stress failure caused by alternating operational loads is the one of important damage mechanisms in the nuclear power plants. To evaluate the thermal stress responses, the Green's function approach has been generally used. In this paper, a method to consider varying heat transfer coefficients when using the Green's function method is proposed by using artificial parameter method and superposition principle. Time dependent heat transfer coefficient has been treated by using a modified fluid temperature and a constant heat transfer coefficient. Three-dimensional temperature and stress analyses reflecting entire geometry and heat transfer properties are required to obtain accurate results. An efficient and accurate method is confirmed by comparing its result with corresponding 3D finite element analysis results for a reactor pressure vessel (RPV). From the results, it is found that the temperature dependent material properties and varying heat transfer coefficients can significantly affect the peak stresses and the proposed method can reduce computational efforts with satisfactory accuracy.

1. Introduction

Thermal stress failure caused by alternating operational loads is the one of important damage mechanisms in the nuclear power plants. The design of major nuclear components for the prevention of fatigue failure has been performed on the basis of ASME codes, which are usually very conservative. The sustained interest in the area of remaining life prediction arises from the need to avoid costly outages and safety considerations and to extend the plant operation life. So, it is very important to monitor the degradation due to thermal fatigue in order to keep the integrity of major components during the long term operation. The important step in online fatigue monitoring is the conversion of plant transients to the stress responses in the components.

A largely used methodology of stress-based fatigue monitoring is the Green's Function Technique (GFT), which is an effective method for online fatigue monitoring system with a fast algorithm to calculate the thermal stresses corresponding to actual operating data acquired from sensors. The time histories of the outputs are evaluated from the time histories of the inputs by solving a set of convolution integrals. The only data necessary to perform the calculation are the Green's functions of the thermomechanical model, that is, time histories of thermal stresses due to unit step inputs. Many researchers [1–5] have shown that the temperature responses and thermal stresses can be estimated using GFT. In [6], the approximate analytical models of temperature and thermal stress in a two-dimensional axis-symmetry object are presented by using multiple parameter perturbation method, which can deal with temperature-dependent properties having small parameters. In [7], a methodology is proposed to consider the temperature-dependent material properties having no small parameters using the artificial parameter method. However, the nonlinear problem caused by varying heat transfer coefficients has not been solved. In [8], temperatures at the boundaries of the model are evaluated by using a FE model and thermal stress is computed by means of

the GFT as response to variations of such boundary temperatures to deal with varying heat transfer coefficients, but FE model is still complicate and time consuming.

Since few currently available online fatigue monitoring systems adopting a conventional GFT algorithm can treat the nonlinear thermoelastic problems of a three-dimensional object caused by temperature-dependent properties together with varying heat transfer coefficients, to reduce the computational efforts, in this paper, Green's function approach to the temperature and stresses in a three-dimensional object are introduced. Varying heat transfer coefficients are simplified by the Lagrange polynomial functions. Using the artificial parameter method, nonlinear problems resulting from temperature-dependent material properties and varying heat transfer coefficients have been treated. The method using a modified fluid temperature to obtain a constant heat transfer coefficient instead of the real fluid temperature and time dependent heat transfer coefficient is presented to treat the time dependent heat transfer coefficients. Compared with the results obtained through FEM method, our models are shown to have satisfactory accuracy. The proposed models are used for online monitoring the temperatures and thermal stresses of a reactor pressure vessel.

2. Linearization of Nonlinear Differential Equation

The temperature distribution in a reactor pressure vessel satisfies this three-dimensional nonlinear differential equation during a transient thermal conduction process with temperature dependent properties:

$$\begin{aligned}\rho c\frac{\partial T}{\partial t} &= \frac{\partial}{\partial x}\left(\lambda\frac{\partial T}{\partial x}\right)+\frac{\partial}{\partial y}\left(\lambda\frac{\partial T}{\partial y}\right)+\frac{\partial}{\partial z}\left(\lambda\frac{\partial T}{\partial z}\right)\\ &= \nabla\cdot(\lambda\nabla T),\end{aligned} \tag{1}$$

where T is temperature in object, λ is thermal conductivity, ρ is density, c is specific heat, t is time, x, y, z are coordinate variables, and $\nabla\cdot, \nabla$ are the three-dimensional divergence and gradient operators.

The initial temperature of an object is assumed uniform. The boundary conditions are

$$\lambda\frac{\partial T}{\partial n}\bigg|_{\text{boi}} = h(T,t)\left(T_{\text{boi}}-T\right), \tag{2}$$

where boi is the ith surface, T_{boi} is the boundary temperature on the ith surface, ΔT_{boi} is the boundary temperature increment on the ith surface, and $h(T,t)$ is the heat transfer coefficient on the ith surface and can be obtained based on the dimensionless numbers: Reynolds, Grashof, Prandtl, and Nusselt numbers. The fluid parameters and boundary conditions, for example, fluid pressure, density, fluid temperature, and surface temperature are involved in these dimensionless numbers, it is the function of time t and surface temperature T.

When the temperature changes moderately, the stresses analysis can be performed followed by the nonlinear transient thermal analysis. From thermoelastic theory, the isotropic material object satisfies the following equations related with temperature:

$$\begin{aligned}\sigma_x &= \frac{E}{(1-2\nu)(1+\nu)}\left[(1-\nu)\varepsilon_x+\nu\left(\varepsilon_y+\varepsilon_z\right)\right]-\frac{E\beta}{1-2\nu}T,\\ \sigma_y &= \frac{E}{(1-2\nu)(1+\nu)}\left[(1-\nu)\varepsilon_y+\nu\left(\varepsilon_x+\varepsilon_z\right)\right]-\frac{E\beta}{1-2\nu}T,\\ \sigma_z &= \frac{E}{(1-2\nu)(1+\nu)}\left[(1-\nu)\varepsilon_z+\nu\left(\varepsilon_x+\varepsilon_y\right)\right]-\frac{E\beta}{1-2\nu}T,\\ \tau_{xy} &= \frac{E}{2(1+\nu)}\gamma_{xy},\qquad \tau_{yz}=\frac{E}{2(1+\nu)}\gamma_{yz},\\ \tau_{xz} &= \frac{E}{2(1+\nu)}\gamma_{xz},\end{aligned} \tag{3}$$

where E is young's modulus, β is thermal expansion coefficient, ν is Poisson's ratio, σ_x, σ_y, σ_z, τ_{xy}, τ_{yz}, and τ_{xz} are the components of thermal stresses.

Since temperature-dependent material properties such as thermal expansion coefficient, thermal conductivity, young's modulus, and specific heat have been treated and introduced in [6, 7], the following analysis only consider temperature-dependent heat transfer coefficient.

Using the Lagrange polynomial functions, the heat transfer coefficient $h(T,t)$ can be simplified and expressed as follows by means of temperature interpolation:

$$\begin{aligned}h(T,t) &= \sum_{j=0}^{\infty}h(T,t)\bigg|_{T=T_j}\prod_{i=0}^{\infty}\frac{\left(T-T_j'\right)}{\left(T_i'-T_j'\right)}\\ &= h_0(t)+h_1(t)T+h_2(t)T^2+\cdots,\quad i\neq j,\end{aligned} \tag{4}$$

where T_i', T_j' are collocation temperature nodes, $h_{i0}(t)$, $h_{i1}(t)$, $h_{i2}(t)$ are the functions of time t.

The artificial parameter method is used to solve the nonlinear problems in this paper. The artificial parameter method does not require the presence of a small parameter in the nonlinear ordinary differential equation. The method can obtain approximate solutions of nonlinear ordinary differential equations by introducing an artificial parameter in the equations and assuming that the solutions can be expanded in terms of this artificial parameter [9–11].

Substituting (4) into (1), introducing an artificial parameter ζ so that (1) becomes

$$\begin{aligned}&\rho c\frac{\partial T}{\partial t}-\nabla\cdot(\lambda\nabla T)\\ &\quad=0\\ &\text{with }\lambda\frac{\partial T}{\partial n}\bigg|_{\text{boi}}-h_0(t)\left(T_{\text{boi}}-T\right)-h_1(t)T_{\text{boi}}T\\ &\qquad+\zeta\sum_{j=1}^{\infty}\left[\lambda T^j\frac{\partial T}{\partial n}\bigg|_{\text{boi}}+h_j(t)T^{j+1}-h_{j+1}T_{\text{boi}}T^{j+1}\right]\\ &\quad=0,\quad T|_{t=0}=0,\end{aligned} \tag{5}$$

where $\zeta\in[0,1]$ and (5) coincides with (1) for $\zeta=1$.

The solutions of temperature for the nonlinear problem can be written as analytical function of ζ according to the theory of perturbation:

$$T = T_0 + \varsigma T_1 + \cdots = \sum_{j=0}^{\infty} \varsigma^j T_j,$$
$$\sigma = \sigma_0 + \varsigma \sigma_1 + \cdots = \sum_{j=0}^{\infty} \varsigma^j \sigma_j. \tag{6}$$

Substituting (6) into (2) and (5), inducing the terms which have the same power of ζ, we can get the following linear heat transfer problem:

$$\zeta^0 : \rho c \frac{\partial T_0}{\partial t} = \lambda \nabla^2 T_0 \quad \text{with } \lambda_0 \frac{\partial T_0}{\partial n_i}\bigg|_{\text{boi}} = h_0' (t) \left(T_{\text{boi}}' - T_0\right),$$
$$\sigma_{x0} = \frac{E}{(1-2\nu)(1+\nu)} \left[(1-\nu)\varepsilon_{x0} + \nu\left(\varepsilon_{y0} + \varepsilon_{z0}\right)\right] - \frac{E\beta}{1-2\nu} T_0,$$
$$\sigma_{y0} = \frac{E}{(1-2\nu)(1+\nu)} \left[(1-\nu)\varepsilon_{y0} + \nu\left(\varepsilon_{x0} + \varepsilon_{z0}\right)\right] - \frac{E\beta}{1-2\nu} T_0,$$
$$\sigma_{z0} = \frac{E}{(1-2\nu)(1+\nu)} \left[(1-\nu)\varepsilon_{z0} + \nu\left(\varepsilon_{x0} + \varepsilon_{y0}\right)\right] - \frac{E\beta}{1-2\nu} T_0,$$
$$\tau_{xy0} = \frac{E}{2(1+\nu)} \gamma_{xy0}, \qquad \tau_{yz0} = \frac{E}{2(1+\nu)} \gamma_{yz0}, \qquad \tau_{xz0} = \frac{E}{2(1+\nu)} \gamma_{xz0},$$
$$\zeta^1 : \rho c \frac{\partial T_1}{\partial t} = \lambda \nabla^2 T_1 \quad \text{with } \lambda_0 \frac{\partial T_1}{\partial n_i}\bigg|_{\text{boi}} = h_1' (t) \left[-T_1 + T_{\text{boi}}''\right],$$
$$\sigma_{x1} = \frac{E}{(1-2\nu)(1+\nu)} \left[(1-\nu)\varepsilon_{x1} + \nu\left(\varepsilon_{y1} + \varepsilon_{z1}\right)\right] - \frac{E\beta}{1-2\nu} T_1,$$
$$\sigma_{y1} = \frac{E}{(1-2\nu)(1+\nu)} \left[(1-\nu)\varepsilon_{y1} + \nu\left(\varepsilon_{x1} + \varepsilon_{z1}\right)\right] - \frac{E\beta}{1-2\nu} T_1,$$
$$\sigma_{z1} = \frac{E}{(1-2\nu)(1+\nu)} \left[(1-\nu)\varepsilon_{z1} + \nu\left(\varepsilon_{x1} + \varepsilon_{y1}\right)\right] - \frac{E\beta}{1-2\nu} T_1, \tag{7}$$

where

$$h_0' (t) = h_0 (t) - h_1 (t) T_{\text{boi}} (t),$$
$$T_{\text{boi}}' (t) = \frac{h_0 (t)}{h_0 (t) - h_1 (t) T_{\text{boi}} (t)} T_{\text{boi}} (t),$$
$$T_{\text{boi}}' (t) = \frac{h_1 (t) T_0^2 - h_2 (t) T_0^2 T_{\text{boi}} (t) - h_0' (t) T_0 \left(T_{\text{boi}}' - T_0\right)}{h_0 (t) - h_1 (t) T_{\text{boi}} (t)}. \tag{8}$$

Thus, the nonlinear thermoplastic problem has been linearized. After linearized the governing equations using artificial parameter method, one can calculate directly temperature by GFT.

3. Time Dependent Heat Transfer Coefficients

Though (7) can be calculated directly by means of GFT, it is difficult to evaluated Green's function since the heat transfer coefficients are time dependent. In [7], temperatures at the boundaries of the model are evaluated by using a reduced FE model and thermal stress is computed by means of the GFT as response to variations of such boundary temperatures to deal with varying heat transfer coefficients, but FE model is complicate and time consuming. In this paper, we present a different method to treat the time dependent heat transfer coefficients. The key idea is that a modified fluid temperature is used to obtain a constant heat transfer coefficient considering the real fluid temperature and time dependent heat transfer coefficient. Temperatures and thermal stresses are evaluated by a modified fluid temperature and a constant heat transfer coefficient.

The modified fluid temperature meets the following thermal flux conservation equation:

$$h (t) \left(-T + T_{\text{boi}}\right) = h_m \left(-T + Tm_{\text{boi}}\right), \tag{9}$$

where h_m is a modified constant heat transfer coefficient and Tm_{boi} is a modified fluid temperature.

From (9), one can obtain

$$Tm_{\text{boi}} = \frac{h (t) \left(-T + T_{\text{boi}}\right)}{h_m} + T. \tag{10}$$

If h_m is selected, one can obtain the temperatures T at the boundaries of the model by the following equation:

$$T = \sum_i \sum_{\tau=t_D}^{t} \left[G_{\text{boi}} (t-\tau) \Delta Tm_{\text{boi}} (\tau)\right], \tag{11}$$

where $\Delta Tm_{\text{boi}}(t)$ is the ith increment of the modified fluid temperature; $G_{\text{boi}}(t)$ is the temperature step responses on the surface at and time t when inputting step signal and a constant heat transfer coefficient h_m.

From (10) and (11), one can obtain the modified fluid temperature, accordingly, temperatures and thermal stresses at any point are evaluated by the modified fluid temperature and the constant heat transfer coefficient.

Table 1: Materials properties of the cylinder.

λ (W/m/°C)	ρ (Kg/m^3)	C (J/Kg/°C)	$\beta * 10^{-5}$ (1/°C)	E (GPa)
37.4	7800	417	1.0344	214.5

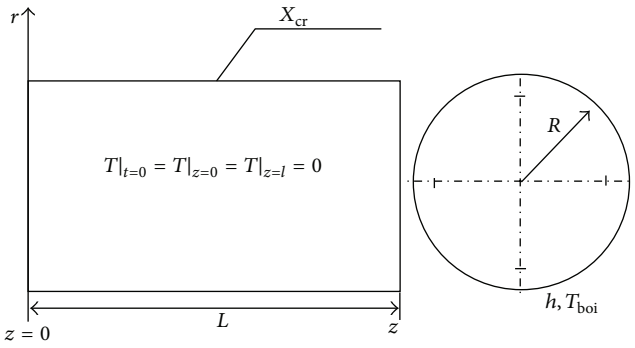

Figure 1: Geometry and boundary conditions of the cylinder.

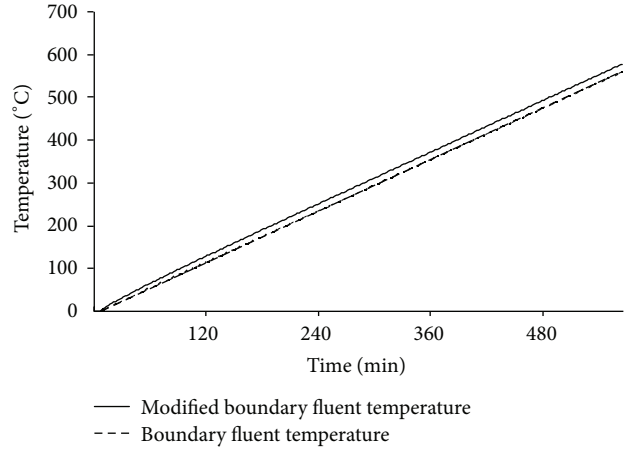

Figure 2: Time histories of boundary fluid temperatures for h = 8000 and modified boundary fluid temperatures for h = 800.

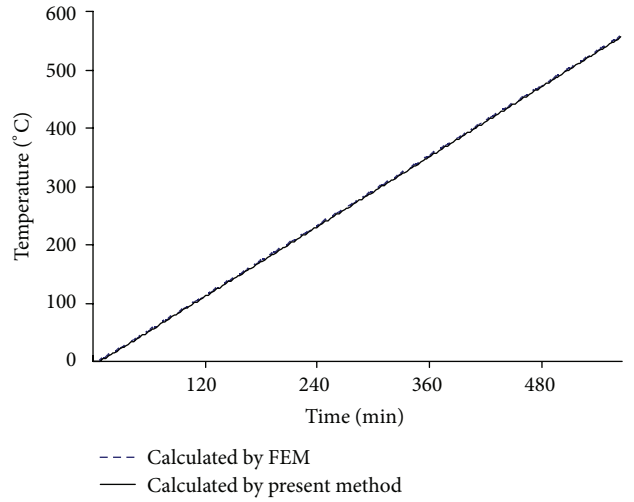

Figure 3: Time histories of temperatures calculated by FEM for h = 8000 and present method using modified boundary fluid temperatures for h = 800 at critical point.

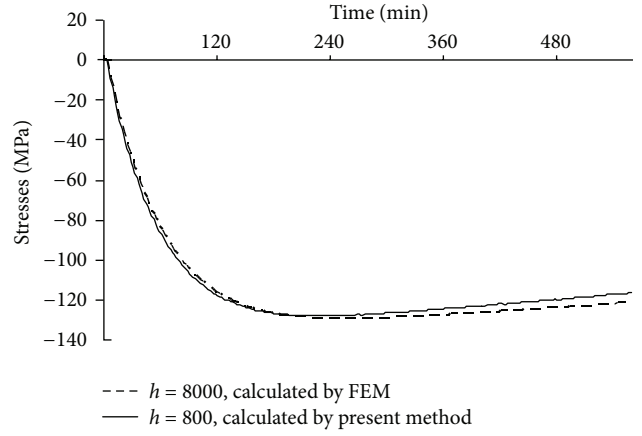

Figure 4: Time histories of axial stresses calculated by FEM for h = 8000 and present method using modified boundary fluid temperatures for h = 800 at critical point.

To verify the accuracy of temperatures and thermal stresses evaluated by the modified fluid temperature and the constant heat transfer coefficient, the temperature and thermal stress calculations of a cylinder were performed by using the present method.

Geometrical dimensions and boundary conditions of the cylinder are plotted in Figure 1. The radius of the cylinder is 0.5 m, the length is 2 m, the initial temperature is assumed as 0°C.

The heat transfer coefficients considered are 8000 W/m^2/°C and 80 W/m^2/°C, the modified heat transfer coefficient is constant and equal to 800 W/m^2/°C.

Time histories of fluid temperatures on the outer surfaces are rising at the rate of 1°C/min during 560 minutes. The point calculated is selected at the coordinate Xcr(r = 0.5, z = 1.05). Material properties of the cylinder are listed in Table 1.

Figure 2 shows time histories of boundary fluid temperatures for h = 8000 and modified boundary fluid temperatures for h = 800. Figure 3 shows time histories of temperatures calculated by FEM for h = 8000 and present method using modified boundary fluid temperatures for h = 800 at the critical point.

Figure 4 shows time histories of axial stresses calculated by FEM for h = 8000 and present method using modified boundary fluid temperatures for h = 800 at the critical point. Figure 5 shows time histories of tangential stresses calculated by FEM for h = 8000 and present method using modified boundary fluid temperatures for h = 800 at the critical point.

Figure 6 shows time histories of boundary fluid temperatures for h = 80 and modified boundary fluid temperatures for h = 800. Figure 7 shows time histories of temperatures calculated by FEM for h = 80 and present method using modified boundary fluid temperatures for h = 800 at the critical point.

Figure 8 shows time histories of axial stresses calculated by FEM for h = 80 and present method using modified

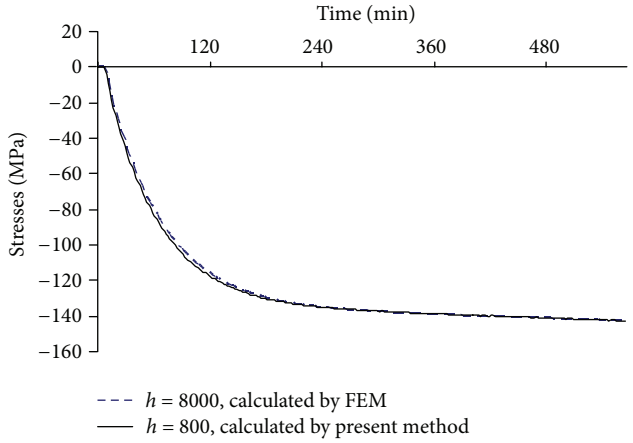

Figure 5: Time histories of tangential stresses calculated by FEM for $h = 8000$ and present method using modified boundary fluid temperatures for $h = 800$ at critical point.

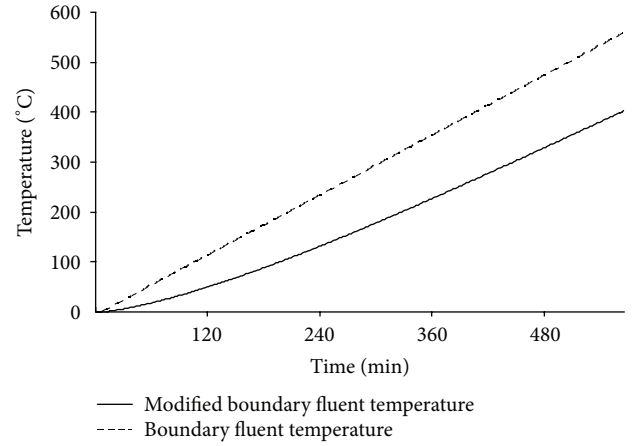

Figure 6: Time histories of boundary fluid temperatures for $h = 80$ and modified boundary fluid temperatures for $h = 800$.

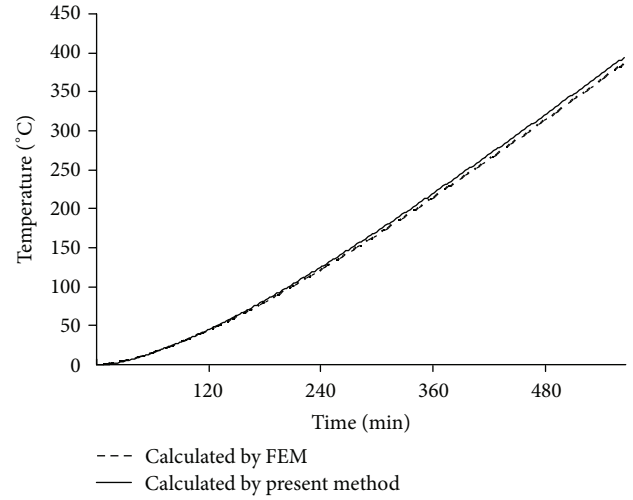

Figure 7: Time histories of temperatures calculated by FEM for $h = 80$ and present method using modified boundary fluid temperatures for $h = 800$ at critical point.

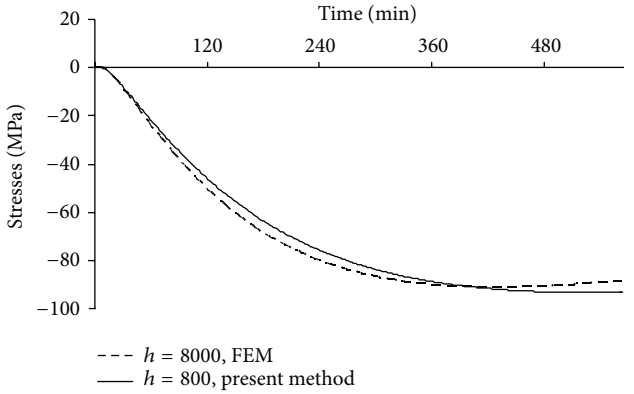

Figure 8: Time histories of axial stresses calculated by FEM for $h = 80$ and present method using modified boundary fluid temperatures for $h = 800$ at critical point.

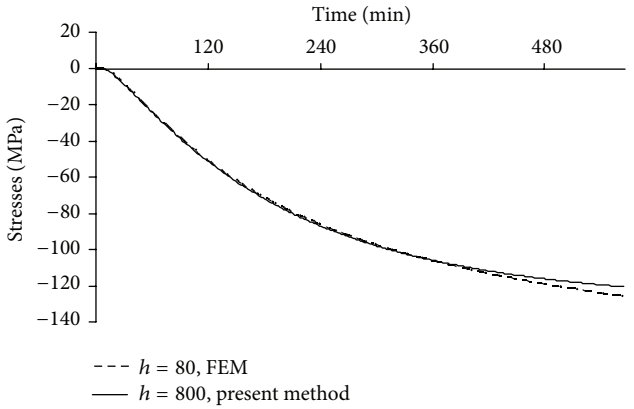

Figure 9: Time histories of tangential stresses calculated by FEM for $h = 80$ and present method using modified boundary fluid temperatures for $h = 800$ at critical point.

boundary fluid temperatures for $h = 800$ at the critical point. Figure 9 shows time histories of tangential stresses calculated by FEM for $h = 80$ and present method using modified boundary fluid temperatures for $h = 800$ at the critical point.

In the two cases, the temperatures and thermal stresses obtained by the model using the modified fluid temperature and the modified heat transfer coefficient agree well with those calculated by FEM using the original heat transfer coefficients and fluid temperature.

4. Result Comparisons and Application

The proposed models can be used for online monitoring the temperatures and thermal stresses of a reactor pressure vessel.

Figure 10 shows a typical three-dimensional RPV model in a nuclear power plant and employed in the present work. The finite element model was prepared to get the temperature and stress variation at concerned regions.

As shown in Figure 10, the RPV considered is that of a 4-loop PWR with an internal diameter of 5000 mm, a wall

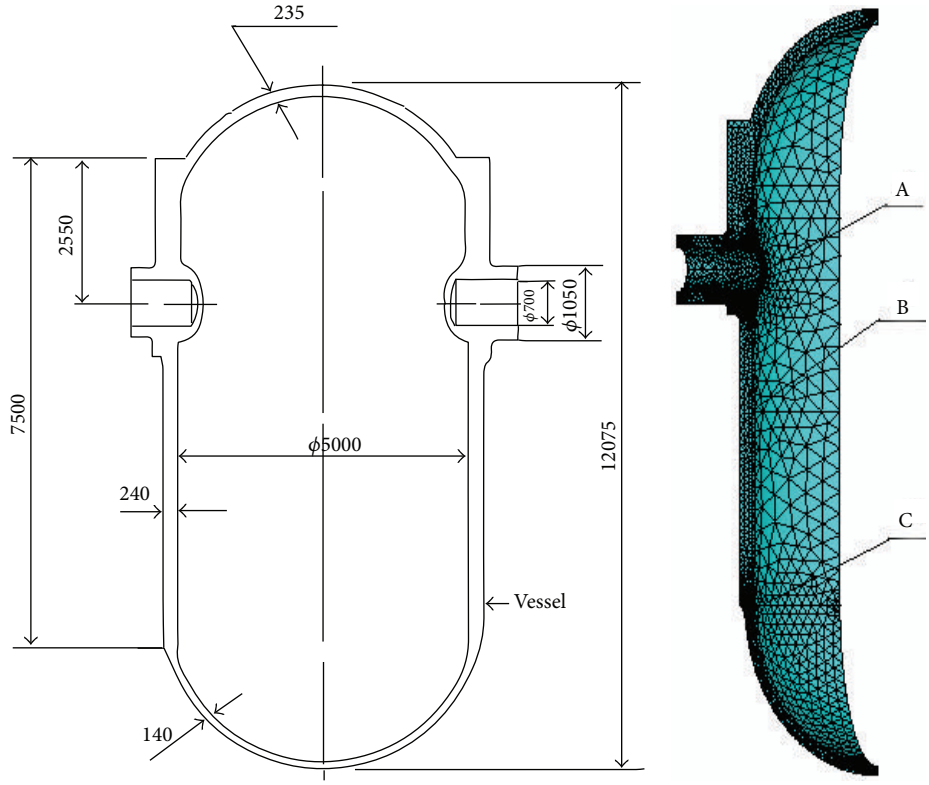

Figure 10: A three-dimensional finite element model showing critical points and geometrical dimensions.

Table 2: Materials properties of RPV.

Temperature (°C)	λ (W/m/°C)	ρ (Kg/m^3)	C (J/Kg/°C)	$\beta * 10^{-5}$ (1/°C)	E (GPa)
20	45.4	7800	450	1.0344	204.1
100	44.4	7800	490	1.13	196.3
200	43.2	7800	520	1.23	188.6
300	41.8	7800	560	1.34	180.2

thickness of 240 mm. One symmetrical slice of 45° out of 360° of the full model is used. The RPV was made of 22NiMoCr37.

The material properties considered in the present analysis are shown in Table 2. The analysis was performed by using the general-purpose finite element program, ANSYS. Solid87, and 92 models, 3-D 10-Node Tetrahedral thermal, and structural solids are adopted in this paper. In order to evaluate the quantitative difference between FEM and the present method analyses, Temperature and thermal stress results are compared in 3 critical points A, B, and C, as shown in Figure 10.

Figure 11 shows a typical heat-up and cool-down transient operation. Time histories of fluid temperatures on the inner surfaces are rising at the rate of 2°C/min from 0°C during 150 minutes, holding on during the following 180 minutes, and then dropping to 0°C during 120 minutes.

The varying heat transfer coefficients are taken as a linear increase from 600 W/m^2/°C to 800 W/m^2/°C for convenience, the modified heat transfer coefficient is taken as a const and

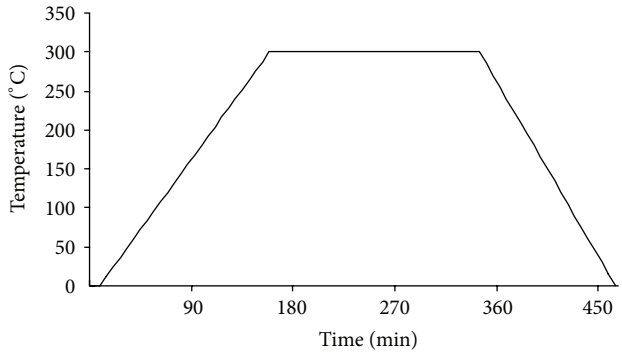

Figure 11: Time histories of boundary fluid temperatures.

equals to 800 W/m^2/°C. The outer surface of the model is assumed to be thermally insulated. A thermal stress analysis for a unit step change of the boundary temperature time history is performed to calculate Green's functions at the critical

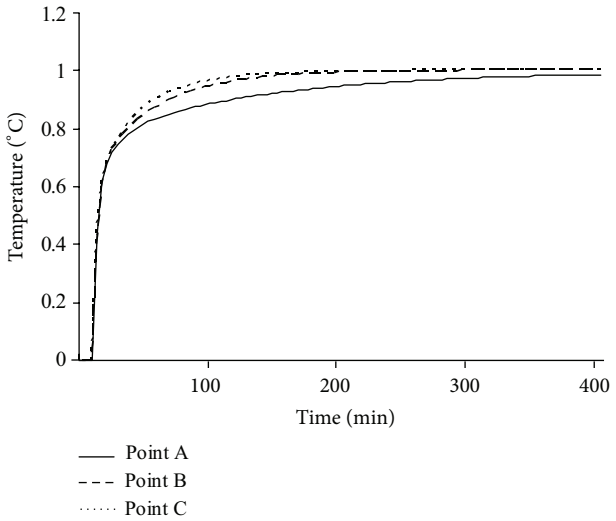

Figure 12: Calculated Green's functions of temperature at critical points A, B and C.

points. The calculated Green's functions of temperature at the critical points for the heat transfer coefficient $h = 800\,\mathrm{W/m^2/^\circ C}$ are presented in Figure 12. Figure 13 shows the calculated Green's functions of the x, y, z, and shear stress components for the heat transfer coefficient $h = 800\,\mathrm{W/m^2/^\circ C}$ at points A, B, and C.

Figure 14 shows the results of temperature errors calculated by FEM with temperature-independent material properties and constant heat transfer coefficients $h = 800\,\mathrm{W/m^2/^\circ C}$ and by the present method with temperature-dependent properties and varying heat transfer coefficients when serving the temperature calculated by FEM with temperature dependent properties and varying heat transfer coefficients as a standard at critical points identified in Figure 10.

Figure 15 presents the comparison results of stress components σ_z calculated by FEM and the method presented. Figure 16 presents the comparison results of von-mises stress calculated by FEM and the method presented.

It is shown obviously that when considering temperature dependent properties and varying heat transfer coefficients, the results have distinct difference with those calculated with constant properties by FEM. However, Results presented in this paper show that the accuracy of stress calculated via the present models are satisfactory. Furthermore, we can get more accurate results when considering the second and higher orders of small parameters.

5. Conclusions

The temperature-dependent material properties and varying heat transfer coefficients have significant effect on the temperature and thermal stresses. Therefore, to monitor fatigue damage by using the Green's function method for real operating conditions in a nuclear power plant, it is required to consider the temperature dependency of the material properties and varying heat transfer coefficients which affect the maximum stress ranges for a fatigue evaluation.

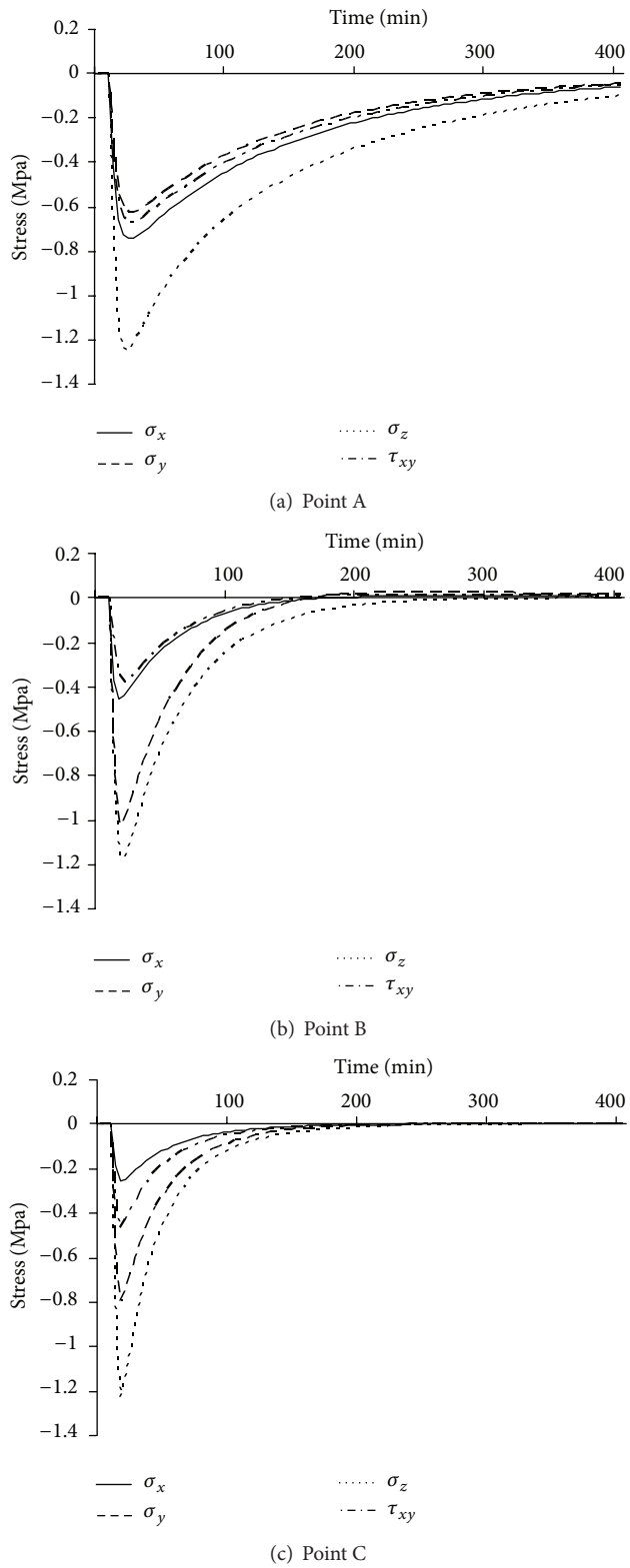

Figure 13: Calculated Green's functions of thermal stresses at critical points A, B, and C.

In this paper, a method to consider temperature-dependent material properties and varying heat transfer coefficients when using the Green's function method is proposed by using

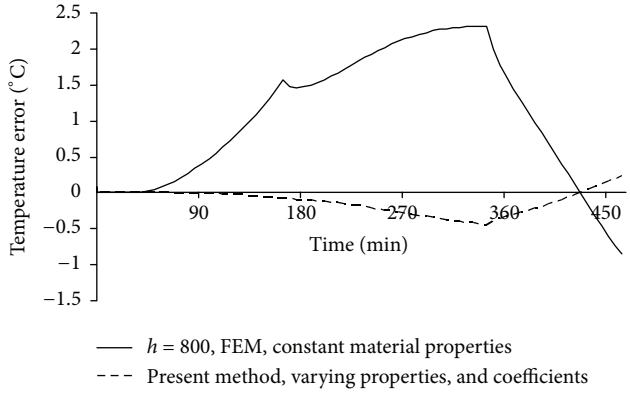

(a) Point A

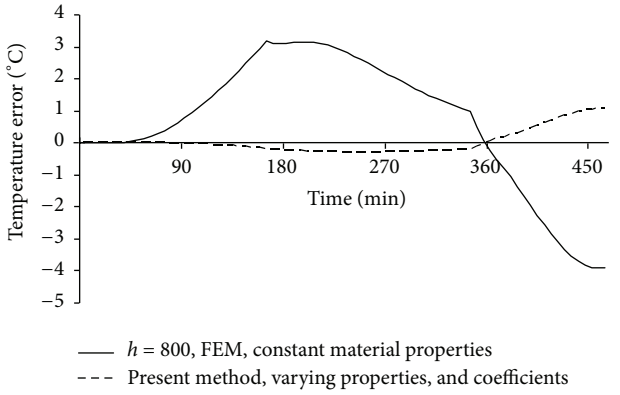

(b) Point B

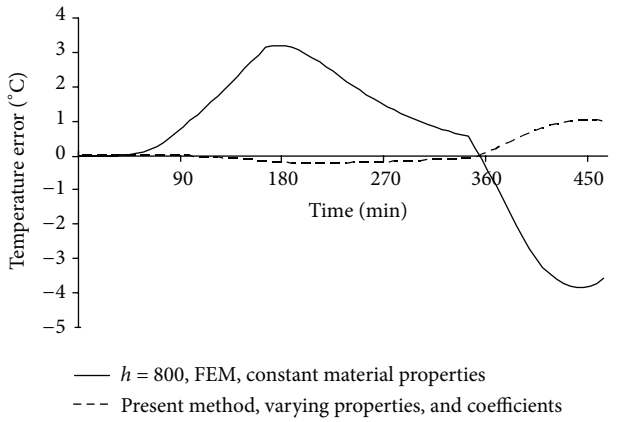

(c) Point C

Figure 14: Temperature errors calculated by FEM with temperature-independent material properties and constant heat transfer coefficients and by the method presented with temperature-dependent properties and varying heat transfer coefficients compared with FEM with temperature-dependent properties and varying heat transfer coefficients at critical points.

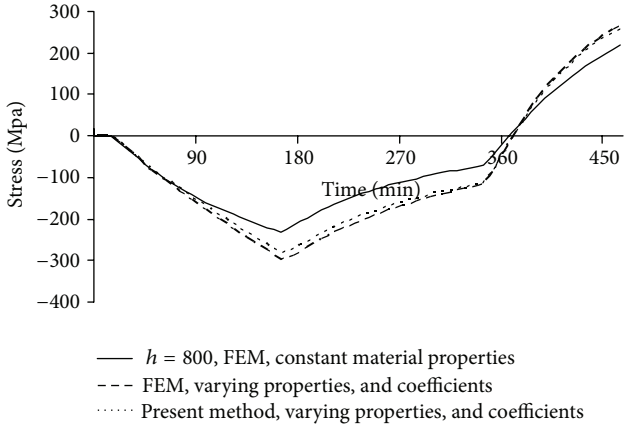

(a) Point A

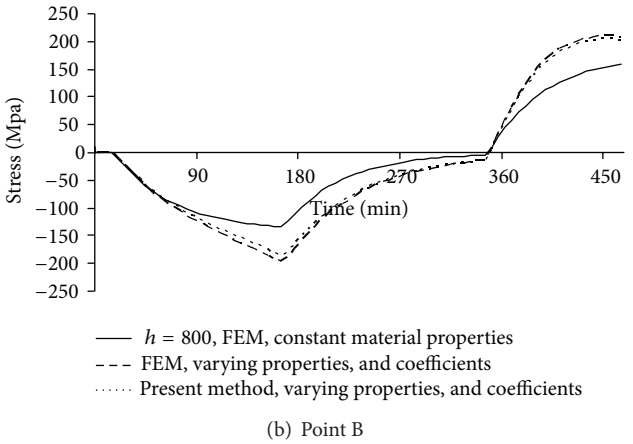

(b) Point B

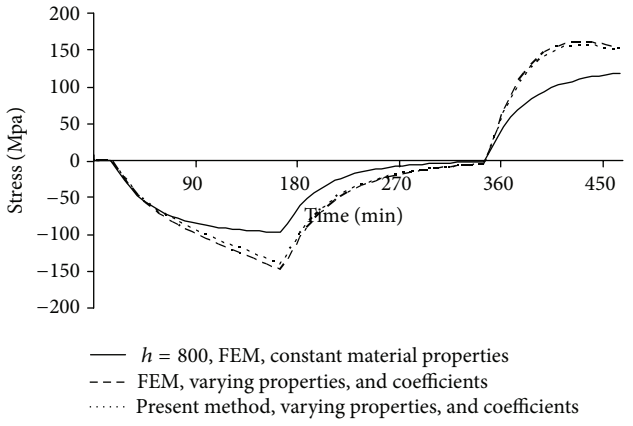

(c) Point C

Figure 15: Stress components σz calculated by FEM with temperature-independent material properties and constant heat transfer coefficients, by the method presented with temperature-dependent material properties and varying heat transfer coefficients and by FEM with temperature-dependent material properties and varying heat transfer coefficients at critical points A, B and C.

artificial parameter method and superposition principle to reduce the computational efforts. Time dependent heat transfer coefficient has been treated by using a modified fluid temperature and a constant heat transfer coefficient. The proposed method is expected to deliver more accurate fatigue life evaluation for the real operating conditions of RPV and, also, applicable to a real-time fatigue monitoring system with high accuracy.

There are still some limitations in the use of the GFT: the severe thermal transient case that could result in a high

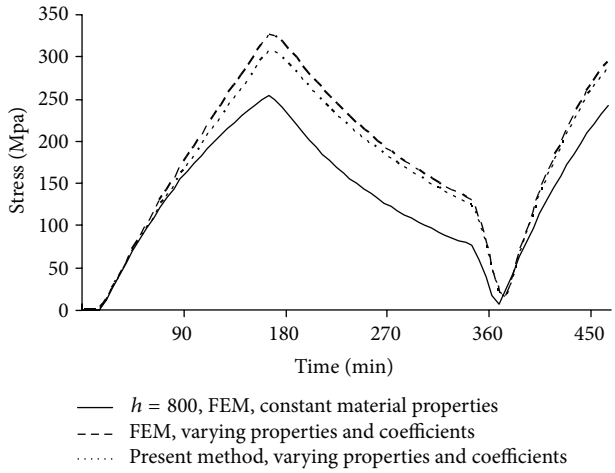

(a) Point A

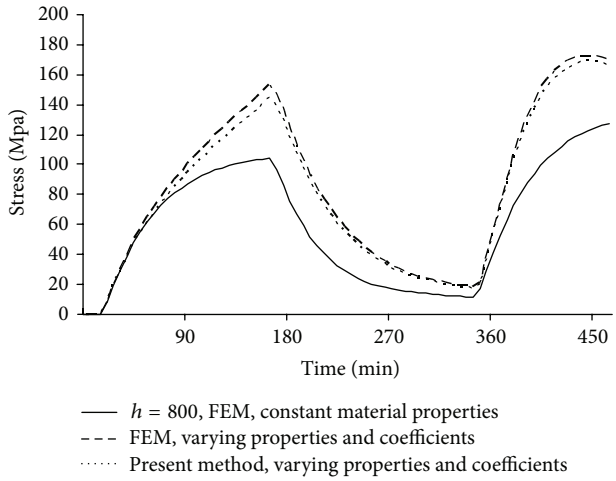

(b) Point B

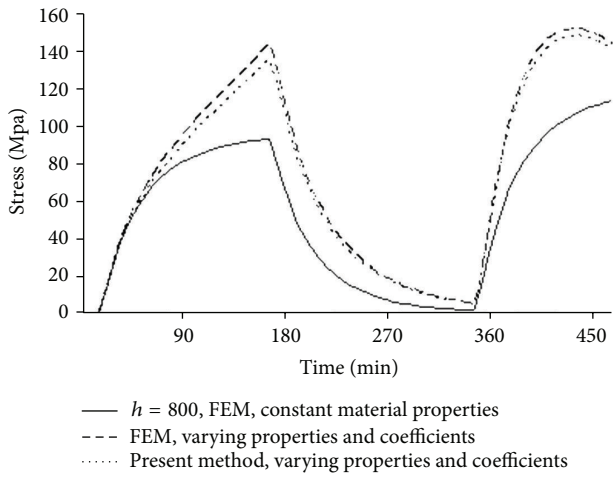

(c) Point C

Figure 16: Von mises stresses calculated by FEM with temperature-independent material properties and constant heat transfer coefficients, by the method presented with temperature-dependent material properties and varying heat transfer coefficients and by FEM with temperature-dependent material properties and varying heat transfer coefficients at critical points A, B and C.

degree of a nonlinear temperature distribution through a wall thickness and the case that actual geometry changes on susceptible regions subject to certain types of degradation mechanisms such as flow accelerated corrosion, erosion, and cracking. The authors plan to conduct further research on the online fatigue monitoring system to solve these problems and performance improvement of the system.

Acknowledgment

This work is partly supported by the National Natural Science Foundation of China (Approval no. 51376140).

References

[1] N. K. Mukhopadhyay, B. K. Dutta, and H. S. Kushwaha, "On-line fatigue-creep monitoring system for high-temperature components of power plants," *International Journal of Fatigue*, vol. 23, no. 6, pp. 549–560, 2001.

[2] S. Zucca, D. Botto, and M. M. Gola, "Faster on-line calculation of thermal stresses by time integration," *International Journal of Pressure Vessels and Piping*, vol. 81, no. 5, pp. 393–399, 2004.

[3] N. K. Mukhopadhyay, B. K. Dutta, H. S. Kushwaha, S. C. Mahajan, and A. Kakodkar, "On line fatigue life monitoring methodology for power plant components," *International Journal of Pressure Vessels and Piping*, vol. 60, no. 3, pp. 297–306, 1994.

[4] G.-H. Koo, J.-J. Kwon, and W. Kim, "Green's function method with consideration of temperature dependent material properties for fatigue monitoring of nuclear power plants," *International Journal of Pressure Vessels and Piping*, vol. 86, no. 2-3, pp. 187–195, 2009.

[5] M. Y. Ahn, J. C. Kim, Y. S. Chang et al., "Development of a Three-Dimensional Green's Function and its Application to the Fatigue Evaluation of Reactor Pressure Vessel," in *Proceedings of the ASME Pressure Vessels and Piping Division Conference (PVP '06)*, pp. 527–532, Vancoucer, Canada, July 2006.

[6] H. Zhang, C. Nie, Y. Xiong, D. Xie, and Y. Yu, "Approximate analytical models of temperature and thermal stresses for 2D axis-symmetry object with temperature-dependent properties," *International Journal of Thermal Sciences*, vol. 53, pp. 100–107, 2012.

[7] H. Zhang, Y. Xiong, C. Nie, D. Xie, and K. Sun, "A methodology for online fatigue monitoring with consideration of temperature-dependent material properties using artificial parameter method," *Journal of Pressure Vessel Technology—Transactions of the ASME*, vol. 134, no. 1, Article ID 011201, 2012.

[8] D. Botto, S. Zucca, and M. M. Gola, "A methodology for on-line calculation of temperature and thermal stress under non-linear boundary conditions," *International Journal of Pressure Vessels and Piping*, vol. 80, no. 1, pp. 21–29, 2003.

[9] H. Zhang, W. Kan, and X. Hu, "Green's function approach to the nonlinear transient heat transfer analysis of functionally graded materials," *International Journal of Thermal Sciences*, vol. 71, pp. 292–301, 2013.

[10] C. M. Bender, K. A. Milton, S. S. Pinsky, and L. M. Simmons Jr., "A new perturbative approach to nonlinear problems," *Journal of Mathematical Physics*, vol. 30, no. 7, pp. 1447–1455, 1989.

[11] M. Senator and C. N. Bapat, "A perturbation technique that works even when the non-linearity is not small," *Journal of Sound and Vibration*, vol. 164, no. 1, pp. 1–27, 1993.